Automotive Science and Engineering, Vol. 14, No. 3, (2024), 4472-4495

Iran University of Science and Technology

Automotive Science and Engineering

Journal Homepage: ase.iust.ac.ir

ISSN: 2008-9899

Role of Nozzle Hole Diameter in Modulating Spray Dynamics and Enhancing Combustion Performance in Reactivity-Controlled Compression Ignition Engines

Mehran Nazemian[1*], Mehrdad Nazemian[2], Mahdi Hosseini Bohloli[3], Hadi Hosseini Bohloli[4], Mohammad Reza HosseiniTazek[5]

[1]Lecturer in the Mechanical Department, Vahdat institute of Higher Education, Torbat-e Jam

[2]Master's degree graduate, Mechanical Engineering, Sahand University of Technology, Tabriz

[3]Bachelor's degree Student, Vahdat institute of Higher Education, Torbat-e Jam

[4]Bachelor's degree Student, Torbat-e Jam Higher Educational Complex, Torbat-e Jam

[5]Bachelor's degree Student, Vahdat institute of Higher Education, Torbat-e Jam

ARTICLE INFO

Article history:

Received : 17 May 2024

Accepted: 27 Aug 2024

Published: 27 Sep 2024

Keywords:

RCCI Engine

Nozzle Hole Diameter

Spray Dynamics

Combustion Efficiency

Emissions

A B S T R A C T

This study investigates the influence of nozzle hole diameter (NHD) variations on spray dynamics, combustion efficiency, and emissions in a Reactivity-Controlled Compression Ignition (RCCI) engine using Computational Fluid Dynamics (CFD) simulations with the CONVERGE software. The study systematically examines NHDs ranging from 130 µm to 175 µm and evaluates their impact on key parameters such as injection pressure, droplet formation, Sauter Mean Diameter (SMD), and evaporation rates. The results demonstrate that reducing NHD to 130 µm significantly enhances fuel atomization by reducing SMD to 15.49 µm and increasing droplet number by 24%, which in turn accelerates evaporation and improves fuel-air mixing. These effects shorten ignition delays, accelerate combustion, and increase peak cylinder pressures and temperatures. Optimal NHDs (150–160 µm) achieve the highest combustion efficiency (92.04%) and gross indicated efficiency (38.58%). However, further reduction in NHD below this range causes premature ignition, energy dissipation, and higher NOx emissions (10.08 g/kWh) due to elevated combustion temperatures. Conversely, when the NHD increases to 175 µm, the larger droplets formed result in prolonged ignition delays, slower combustion, and lower peak pressures. These effects negatively impact combustion efficiency and promote incomplete combustion, leading to higher HC (15.27 gr/kWh) and CO (4.22 gr/kWh) emissions. Larger NHDs, however, lower NOx emissions to 2.66 gr/kWh due to reduced peak temperatures. This study clearly identifies an optimal NHD range (150–160 µm) that effectively balances droplet size, evaporation rate, combustion timing, and emission reduction, thereby enhancing both engine performance and environmental sustainability.

*Corresponding Author
Email Address: Mehran_nazemian@yahoo.com
https://doi.org/10.22068/ase.2024.694

[DOI: 10.22068/ase.2024.694]

1. Introduction

1.1. Literature review

The Reactivity Controlled Compression Ignition (RCCI) is an advanced dual-fuel combustion method that combines a high-reactivity fuel (such as diesel) with a low-reactivity fuel (such as gasoline or natural gas), improving combustion efficiency and reducing emissions [1, 2].

A key feature of RCCI engines is their ability to operate at lower combustion temperatures, significantly reducing nitrogen oxides (NOx) emissions [1]. Additionally, these engines demonstrate higher gross indicated efficiency (GIE) values, exceeding 49% in certain cases, outperforming conventional diesel engines [3]. However, challenges such as combustion stability and emissions control remain, particularly under varying loads [2, 4].

One of the critical factors in improving the performance and emissions of RCCI engines is the optimization of nozzle hole diameter (NHD), with a focus on spray dynamics. This includes processes such as fuel droplet formation, primary and secondary droplet breakup, droplet collisions, and evaporation, all of which influence fuel-air mixing, combustion efficiency, and emissions.

The NHD in fuel injectors plays a critical role in the engine performance and emissions. Various studies have explored how changes in the nozzle geometry affect the spray characteristics, combustion processes, and exhaust emissions. This literature review synthesizes the findings of articles that investigate the influence of the NHD on diesel engine performance, focusing on aspects such as fuel atomization, combustion efficiency, and the emission of pollutants like NOx, CO, and soot.

Smaller nozzle diameters generally enhance fuel atomization, leading to finer droplets that improve air-fuel mixing. For instance, Tang et al. [5] demonstrated that a NHD of 0.23 mm resulted in reduced spray liquid length and enhanced fuel-air mixing compared with larger diameters. Improved atomization is imperative for efficient combustion and emission reduction. In another study, Andsaler et al. [6] demonstrated that the interaction between the nozzle diameter and the injection pressure is significant. Higher injection pressures can compensate for larger nozzle diameters by increasing the velocity of fuel droplets, thereby enhancing penetration. Conversely, lower diameters at high pressures result in reduced droplet sizes and longer penetration lengths, which are beneficial for combustion.

Som et al. [7] investigated the droplet size distribution. They demonstrated that the Sauter mean diameter (SMD) of the droplets is a pivotal parameter influenced by the nozzle geometry. The use of smaller nozzles results in the formation of smaller droplets, thereby enhancing the evaporation rate and improving the combustion efficiency. In a separate study, Klyus et al. [8] demonstrated that nozzle configurations with reduced diameters result in a more uniform droplet size distribution, which is advantageous for combustion processes. In another study, Liu et al. [9] investigated the impact of varying the nozzle diameter on the combustion characteristics. The nozzle diameter significantly affects the combustion process in diesel engines. Smaller nozzles facilitate better mixing of fuel and air, leading to more complete combustion and higher thermal efficiency. For instance, a study revealed that decreasing the nozzle diameter from 0.16 mm to 0.08 mm led to a substantial reduction in soot emissions, concurrently enhancing combustion efficiency [10].

In other studies, researchers have examined the ignition delay (ID) and flame characteristics with different nozzle diameters. These results demonstrate that the NOD period is influenced by the nozzle diameter. Smaller diameters result in quicker ignition because of enhanced atomization and mixing [5]. Additionally, the flame structure and combustion duration are affected by the nozzle size; smaller nozzles promote a more stable flame and reduce the likelihood of soot formation [11]. In other studies, the effect of the NHD on pollution was examined. The results indicated that smaller nozzle diameters can lead to increased NOx emissions due to higher in-cylinder temperatures

[DOI: 10.22068/ase.2024.694]

[12]. However, the overall trend has shown that optimizing the nozzle geometry can mitigate these emissions while maintaining performance [13]. It was also found that the reduction of soot emissions is a significant benefit of using smaller nozzle diameters. Consequently, these findings underscore the pivotal role of nozzle size optimization in achieving substantial reductions in soot formation, which is a crucial aspect in complying with stringent emission regulations [12, 13].

Wang et al. [14] examined the effects of ultra-high injection pressure and micro-hole nozzles on flame structure and soot formation. The results revealed that the use of micro-hole nozzles led to a substantial reduction in soot emissions, particularly at elevated injection pressures. The authors concluded that the combination of micro-hole nozzles and high injection pressure could effectively mitigate soot formation in diesel engines. Furthermore, the researchers determined that smaller nozzle diameters are associated with lower CO and hydrocarbon (HC) emissions because they promote better combustion and reduce the formation of fuel-rich zones [12]. The findings of these studies show that the selection of the nozzle diameter plays a pivotal role in the mitigation of these emissions while ensuring the combustion efficiency [12].

Yao et al. [15] examined the impact of the nozzle geometry on the spray characteristics and combustion characteristics in a constant-volume combustion chamber. Using high-speed imaging, this study examined the droplet size distribution and combustion heat release rates. The findings indicated that decreasing the nozzle diameter resulted in droplets with a higher surface-area-to-volume ratio, thereby enhancing the combustion efficiency and reducing soot formation. The results underscore the significance of calibrating the nozzle design to adhere to stringent emission regulations while preserving engine performance. Zhao et al. [16] investigated the interaction between the nozzle structure and pre-chamber reactivity in ammonia engines. The results revealed that nozzle diameter exerts a substantial influence on combustion characteristics and emissions. The findings indicate that decreasing nozzle diameter enhanced fuel-air mixing and combustion efficiency, consequently reducing nitrogen-based emissions. The findings underscore the necessity of optimizing nozzle design in alternative fuel engines. Payri et al. [17] established a correlation between the nozzle geometry and the spray characteristics and combustion processes in direct-injection diesel engines. The present study employed chemiluminescence techniques to analyze combustion development. The results indicate that the nozzle conicity and hole diameter influence the liquid phase penetration and combustion efficiency. The authors emphasize the need for precise nozzle designs to enhance combustion performance and reduce emissions. Fu et al. [18] investigated the impact of hydrogen nozzle diameter on the performance of hydrogen-blended methanol engines. The results of this study indicated that decreasing the nozzle diameter enhances the combustion speed and reduces NOD, consequently improving the thermal efficiency. The authors further observed that the diameter of the nozzle had a substantial impact on the emission, with smaller diameters resulting in reduced NOx emissions. Zhang et al. [19] examined the effects of nozzle diameter and swirl ratio on combustion in opposed-piston engines. The results indicate that decreasing the nozzle diameter enhances the droplet size and mixing, thereby improving the combustion efficiency. The researchers recommended specific nozzle diameters and swirl ratios to optimize engine performance. Rojas-Reinoso et al. [20] developed a predictive model for injection rates based on the nozzle geometry of diesel engines. The results demonstrated that variations in the nozzle diameter and hole number significantly affected the injection rate and engine performance. Thus, the authors established a framework for optimizing injector designs with the objective of improving fuel efficiency and reducing emissions. Lahane et al. [21] investigated the effect of the nozzle geometry on the combustion characteristics of a dual-fuel engine. The results indicate that the nozzle design significantly affects the combustion efficiency and emissions. The authors emphasize the need for tailored nozzle configurations to improve the performance of dual-fuel engines.

[DOI: 10.22068/ase.2024.694]

To optimize the combustion process, researchers have increasingly focused on one of the most critical parameters: the fuel droplet size distribution (SMD) throughout the combustion cycle. In particular, it is essential to analyze the maximum and minimum SMD points, especially in relation to the crank angle (CAD) and their variations with respect to NHD. Extensive studies have revealed two critical SMD points, the maximum and minimum values, that play a pivotal role in determining the combustion quality. Previous research emphasizes the importance of selecting appropriate points for SMD analysis, as this significantly influences both combustion efficiency and emissions. In certain studies, the points selected during the early stages of injection (prior to the initial peak of the SMD) have been found to optimize the processes of fuel vaporization and air-fuel mixing. This selection becomes even more crucial in RCCI engines, which operate with multiphase fuels and involve more complex combustion mechanisms.

Research indicates that the SMD, which characterizes the average droplet size in a spray, significantly influences the combustion process. Smaller SMD values generally enhance the vaporization and mixing of fuel with air, thereby improving combustion efficiency and reducing emissions [22, 23].

In RCCI engines, where fuel injection strategies are pivotal, the timing and conditions of injection can critically affect the SMD and, consequently, the combustion characteristics. For instance, studies have shown that optimizing the injection rate and timing can lead to improved mixing and combustion efficiency, as well as reduced pollutant emissions [22, 24]. The initial stages of fuel injection, particularly before the peak injection pressure, are crucial for achieving optimal vaporization and mixing. This is supported by findings that indicate the vaporization process in high-pressure fuel injection systems is primarily mixing-controlled rather than limited by interphase transport rates [25, 26].

Moreover, the impact of fuel properties, such as temperature and pressure, on SMD is significant. Research has demonstrated that increasing the fuel temperature can lead to a larger SMD, which may adversely affect combustion efficiency if not managed properly [27]. Conversely, high injection pressures have been shown to enhance spray dispersion and reduce SMD, which is beneficial for improving combustion characteristics [26]. This interplay between fuel properties and injection parameters underscores the importance of selecting the right points for SMD analysis to optimize the combustion process in RCCI engines.

In conclusion, the careful selection of SMD measurement points, particularly during the initial stages of fuel injection, is essential for optimizing combustion efficiency and emissions in RCCI engines. This optimization is influenced by various factors, including injection timing, fuel properties, and the specific characteristics of the spray, which collectively determine the effectiveness of the combustion process

1.2. Gaps and needs

According to the existing literature, the modification of the nozzle hole diameter is a fundamental parameter for emission control in high-temperature combustion engines, such as SI and CI engines. Consequently, most research efforts have been directed toward the development of high-temperature combustion strategies. This approach has limited the scope of the literature to a limited number of cases, thereby missing the opportunity to identify potentially superior geometries that may exist outside of the cases studied. Another significant gap in the existing literature is the lack of a comprehensive understanding of the processes involved in the quality and quantity of fuel droplets generated before and after combustion. The control of the fuel droplet size distribution is a critical aspect of improving engine efficiency and minimizing emissions. Variables such as fuel viscosity, surface tension, and chemical composition exert a significant influence on fuel droplet size distribution and overall spray quality. As a result, the strategic manipulation of these parameters has emerged as a key way to control the fuel size distribution and thereby facilitate the optimization of combustion processes. Integrating detailed models that elucidate fuel atomization and spray

[DOI: 10.22068/ase.2024.694]

characteristics allows engineers to refine engine design parameters, enabling more efficient combustion processes and reduced emissions. In addition, as emerging technologies such as microfluidics offer promising avenues for manipulating fuel atomization at the microscale, the discovery of the necessary characteristics of optimal fuel droplets for improved combustion has the potential to initiate interdisciplinary collaborations among experts in fluid dynamics, combustion science, and atmospheric chemistry and physics to best address the multifaceted challenges.

1.3. Novelty

The novelty and significance of this study lie in its targeted approach to addressing gaps in engine performance and emission reduction. In this research, the fuel injection process, spray quality, and fuel droplet size distribution are examined by varying the nozzle hole diameters of the engine, aiming to identify their roles in combustion dynamics, engine efficiency, and emission levels. By comparing the results from different variations, the study seeks to identify the key characteristics of an effective nozzle hole diameter and derive the optimal nozzle hole diameter for generating fuel droplets with an ideal size distribution based on these characteristics. This process enhances our understanding of engine performance and facilitates informed decision-making in engine design and optimization. Ultimately, this research contributes to the broader goal of reducing emissions and improving the efficiency of internal combustion engines.

Additionally, the novelty of this study lies in its precise focus on selecting measurement points for the mean droplet diameter (SMD), particularly during the initial stages of fuel injection. Optimizing the SMD is essential for achieving more efficient combustion and reducing emissions in RCCI engines. The key factors for this optimization include: the minimum SMD size before the initial peak of the SMD curve and its timing, the maximum droplet number and its formation time, as well as the maximum SMD size and its occurrence time. Identifying and accurately measuring these parameters plays a crucial role in enhancing combustion efficiency and reducing emissions. This approach contributes to a deeper understanding of fuel atomization processes and their impact on engine performance, thus facilitating the development of more efficient and environmentally friendly engine technologies in the future.

2. Problem description and methodology

The engine modeled in this study was a 1.9-liter TDI Volkswagen light-duty engine, which was purchased from the Advanced Power Systems Research Center at the University of Michigan. The VW TDI engine is a 4-cylinder diesel engine equipped with a variable-geometry turbocharger, and its specifications are provided in Table 1. For n-heptane fuel injection into each cylinder, CRDI injectors (described in Table 2) were employed.

Table 1: Features of the engine available at the Advanced Power Systems Research Center at the University of Michigan used in this study.

Parameter	Value
Cylinder arrangement	Inline 4
Cylinder bore/stroke (mm)	79.5/95.5
Geometric Compression ratio	17:1
IVC (aTDC)	-169
EVO (aTDC)	162
Piston bowl	Mexican hat
Max. Power (kW)	66 @ 3750 RPM
Max. Torque (Nm)	210 @ 1900 RPM

[DOI: 10.22068/ase.2024.694]

Table 2: Specifications of the Bosch direct-injection injector for the used engine.

Injector Type	CRDI
Number of holes	6
Nozzle diameter (mm)	0. 165
Included spray angle (°)	144
Injection pressure (bar)	400

In this study, the three-dimensional computational fluid dynamics (CFD) simulation software CONVERGE was employed to model all processes within the RCCI engine from the IVC moment as the intake valve was closed in the chamber teemed with premixed air-methane gas to the EVO moment when the exhaust valve opened to release pollutants. Hence, the n-heptane fuel injection process, including atomization, breakups, and coalescence, was modeled to predict the quality and quantity of fuel droplets in interaction with the air-methane gas. The evaporated and combusted droplets were modeled through a kinetic mechanism comprising 76 species and 464 reactions [28]. The thermodynamic characteristics of the formed species were simulated by solving the continuity, Navier-Stokes, energy, turbulence, and chemical kinetics equations for each computational cell in the temporal domain. The Droplet distinct Model (DDM) [29] was used to simulate the injection process. For spray breakup, the Modified KH-RT models [30, 31] were used. The first breakup occurs when the high-pressure fuel jet initially disintegrates into larger droplets as it exits the injector nozzle, driven by instabilities and interactions with the surrounding premixed air-methane. The second breakup occurs as larger droplets are further fragmented into finer droplets due to aerodynamic forces during their travel through the combustion chamber. Both stages are crucial for achieving a fine fuel mist, which enhances mixing with air, leading to more efficient combustion, better fuel efficiency, and reduced emissions. The applied turbulence model is the RNG k-ε model [32], while the heat transfer process is simulated using the Wall function model of Han and Reitz [32]. The NTC model [30] was used to simulate collisions, with post-collision outcomes [33] further analyzed using the collision outcome model. The interaction between droplets and walls was modeled using the Wall film model [34], and to speed up the runtime, a Multi-zone chemistry solver [35] is implemented. To enhance the geometric accuracy inside the cylinder, a three-dimensional scan is used to model the cylinder chamber, considering the injector locations. The meshing process in the Converge CFD software is performed automatically using the Adaptive Mesh Refinement (AMR) method to enhance the computational accuracy during code execution. A 360° meshing was employed due to the off-center nature of the piston bowl, as shown in Figure 1. The default size of the computational cells was set to 5 mm, resulting in a mesh network of 150,000 cells. In this study, to isolate and precisely evaluate the impact of variations in nozzle hole diameter, all other geometric parameters of the nozzle, along with fuel injection parameters, were maintained constant.

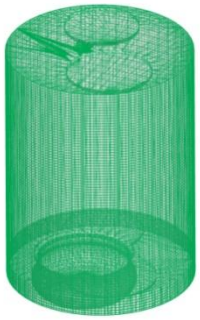

Figure 1: Mesh configuration of combustion chamber.

3. Governing equations

3.1. Conservation relationships

To predict the behavior of fuels and products in fluid and gaseous phases, the required continuity, momentum, energy, and chemical kinetics equations are written as follows [36]:

$$\frac{\partial \rho}{\partial t} + \frac{\partial \rho u_i}{\partial x_i} = S \quad (1)$$

[DOI: 10.22068/ase.2024.694]

$$\frac{\partial \rho u_i}{\partial t} + \frac{\partial \rho u_i u_j}{\partial x_j} = -\frac{\partial P}{\partial x_i} + \rho g_i + \frac{\partial \sigma_{ij}}{\partial x_j} + S_i \quad (2)$$

$$\frac{\partial \rho e}{\partial t} + \frac{\partial u_j \rho e}{\partial x_j} = -P\frac{\partial u_j}{\partial x_j} + \sigma_{ij}\frac{\partial u_i}{\partial x_j} + \frac{\partial}{\partial x_j}\left(K\frac{\partial T}{\partial x_j}\right) + \frac{\partial}{\partial x_j}(\rho D \sum_m h_m \frac{\partial Y_m}{\partial x_j}) + S \quad (3)$$

$$\frac{\partial \rho_m}{\partial t} + \frac{\partial \rho_m u_j}{\partial x_j} = \frac{\partial}{\partial x_j}\left(\rho D \frac{\partial Y_m}{\partial x_j}\right) + S_m \quad (4)$$

where the symbols represent the following physical quantities: u denotes velocity, ρ stands for density, S represents the source term for thermal energy, P is pressure, Y_m indicates the mass fraction of species m, D is the diffusivity coefficient, e is the specific internal energy, K denotes thermal conductivity, h_m is the specific enthalpy, σ_{ij} is the stress tensor, and T represents temperature.

3.2. The relationship between spray dynamics

In this investigation, a Lagrangian drop Eulerian fluid approach was adopted to model the spray dynamics, where the liquid phase was treated as a dispersed phase with physical attributes corresponding to diesel fuel derived from the convergence fluid property library (Tetradecane) [37-42]. These attributes, such as vapor pressure, density, specific heat capacity, and surface tension, can be parameterized as functions of temperature. The modeling of fine droplets in the spray employs a statistical framework using Lagrangian particles termed parcels, which represent ensembles of droplets with similar size characteristics. The Blob injection strategy is implemented in which parcels are stochastically initialized within the nozzle hole with an initial radius equivalent to the nozzle radius, delineating the primary core of the liquid spray. The initialized parcels serve as parent entities constituting the entirety of the liquid spray core. To represent droplet breakup phenomena, a modified Kelvin-Helmholtz-Rayleigh-Taylor (KH-RT) model is employed, comprising distinct stages of primary and secondary breakup [31]. The KH instability model was applied to predict the primary breakup of the injected fuel parcels, while the secondary breakup mechanism, which was attributable to aerodynamic instabilities, was captured through the RT instability model. A schematic depiction of the KH-RT model breakup time is provided in equation 5:

$$\tau_{KH} = \frac{3.726 B_1 R}{\Omega_{KH} \Lambda_{KH}} \quad (5)$$

Where B_1 is an adjustable parameter, and Ω_{KH} and Λ_{KH} represent the frequency and wavelength calculated for the mode with the fastest growth. As evident from Eq. (5), smaller values of B_1 lead to faster breakup, resulting in a higher degree of mixing in the spray process.

The radius of the resulting daughter droplet is calculated as follows:

$$r_c = \frac{\pi C_{RT}}{K_{RT}} \quad (6)$$

Where K_{RT} is the calculated wave number and C_{RT} is an adjustable parameter, typically set to a value of 0.1. This parameter significantly influences the distribution of fuel vapor in the cylinder. The smaller values of C_{RT} result in the production of smaller droplets, leading to their rapid evaporation and consequently contributing to the generation of a higher premixed content.

3.3. Energy relationships

The gross indicated efficiency is calculated from the produced work ($\boldsymbol{W_{gross}}$) and power ($\boldsymbol{P_{gross}}$) as follows [39, 40].

$$W_{gross}\left[\frac{kJ}{cycle}\right] = \int_{-180}^{+180} PdV \quad (7)$$

$$P_{gross}[kW] = W_{gross} \times Engine\ Speed[rpm]/120 \quad (8)$$

$$GIE\ (\%) = \frac{W_{gross}}{\dot{m}_{\mathrm{n-heptane}} \times LHV_{\mathrm{n-heptane}} + \dot{m}_{methane} \times LHV_{methane}} \times 100 \quad (9)$$

where the lower heating value of heptane fuel is 3.42 MJ/kg, whereas that of methane fuel is 50 MJ/kg.

[DOI: 10.22068/ase.2024.694]

The combustion efficiency is also assessed as follows:

$$Comb.Effi.(\eta_c) = \frac{\sum HRR}{\dot{m}_{\text{n-heptane}} \times LHV_{\text{n-heptane}} + \dot{m}_{methane} \times LHV_{methane}} \times 100 \quad (10)$$

Where, $\sum HRR$ is the cumulative heat release rate.

The following relationship represents the emission:

$$Emission\ [\frac{gr}{kWh}] = \frac{\dot{m}_{emission}}{Power_{gross}} \quad (11)$$

The combustion start and duration are respectively measured as follows:

Combustion duration = CA90 CA50

Starting point of combustion = CA10

Where CA10, CA50, and CA90 represent the crank angles at which 10%, 50%, and 90% of the fuel is combusted.

4. Results and discussion

4.1. Validation

To validate the proposed CFD model, experimental results obtained from the laboratory of Michigan Technological University's engine facility were used. For the validation of the simulation results, two different operating conditions of the engine were considered, as outlined in Table 3. The engine speed, BMEP (brake mean effective pressure), fuel injection strategy, and EGR level employed in these two operational modes are distinct from each other [41].

Figure 2 illustrates the prediction of the cylinder pressure and heat release rate by the simulation compared with the experimental values for the operational conditions presented in Table 3, showing good agreement with the measured cylinder pressure values. Additionally, Table 4 presents the predicted pollutants and their comparisons with the experimental values. Note that all simulations conducted in this study were based on case (a).

Table 3: Two operating conditions under which the light duty RCCI engine was simulated to validate the employed model.

Parameters	Case a	Case b
Speed (RPM)	1300	1500
BMEP (Bar)	4	5
Diesel flow rate (gr/s)	0.071	0.107
NG flow rate (gr/s)	0.5	0.56
Air flow rate (Kg/h)	60.736	55.95
SOI1/SOI2 (bTDC)	Singles - 20	55/20
Split type (%/%)	Single	70/30
T_IVC (K)	380	378
Common Rail Pressure (bar)	400	400
BR %	89	85
EGR%	0%	20%

Table 4: Validation of the employed model by comparing the simulation results of emissions for the two examined cases with those of the experiment.

Emission	Case a		Case b	
	Exp	Sim	Exp	Sim
NOx (ppm)	860	723	670	1728
HC (ppm)	7800	4165	5300	3314
CO (ppm)	1380	673	1100	563

[DOI: 10.22068/ase.2024.694]

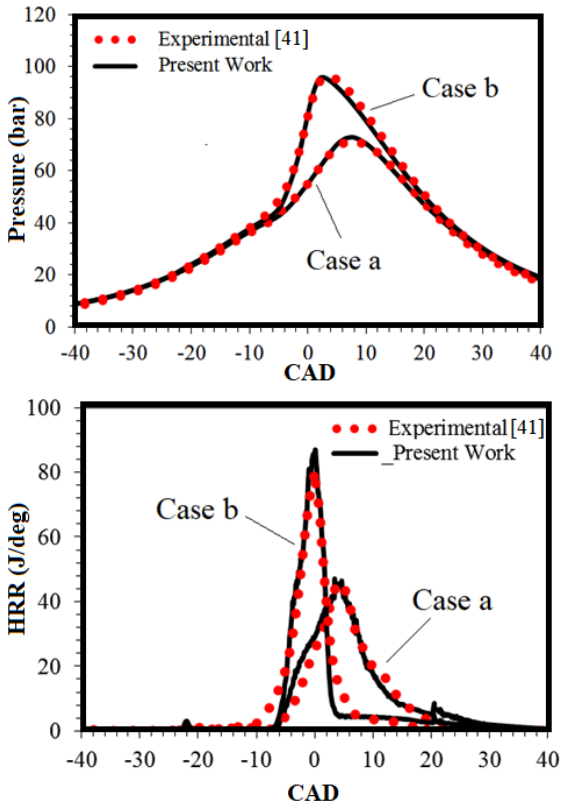

Figure 2: Validation of the in-cylinder pressure and HRR in cases (a) and (b)

4.2. Results

The effect of the NHD on the injection pressure and velocity is a critical aspect of fuel injection systems in internal combustion engines. Studies have indicated that variations in the nozzle geometry have a significant impact on the performance characteristics of injectors, affecting both the injection pressure and velocity of the injected fuel [43-45]. Figure 3 illustrates the effect of NHD on fuel injection pressure and velocity.

The results show that increasing the NHD leads to a decrease in both the injection pressure and fuel injection velocity, whereas decreasing the NHD leads to an increase in these parameters. This behavior can be attributed to the fact that smaller hole diameters increase the hydrodynamic resistance to fuel flow. This increased resistance caused an increase in the upstream pressure behind the nozzle (injection pressure). In addition, larger hole diameters decrease the fuel injection velocity due to the reduction in the injection pressure and the increased cross-sectional area of the flow. Conversely, smaller nozzle diameters produce higher fuel velocities because of the higher injection pressure and smaller cross-sectional area.

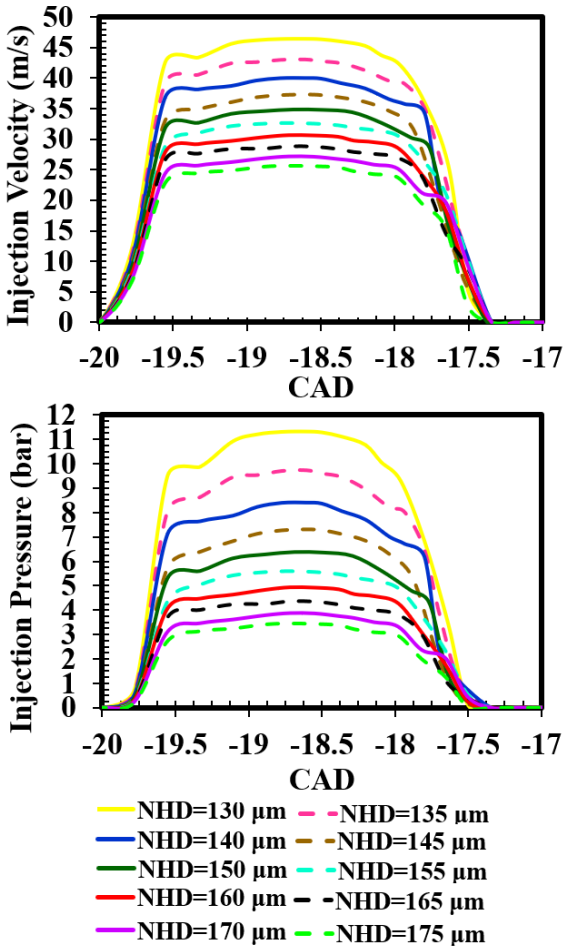

Figure 3: Effect of NHD on injection pressure and velocity.

Figure 4 illustrates the effect of the NHD on Sauter Mean Diameter (SMD). The results indicate that the droplet size decreases as the NHD decreases. This phenomenon occurs due to the increased shear energy and breakup forces in the fuel flow caused by the higher injection pressure and velocity. These forces cause larger droplets to break into smaller droplets. In this scenario, smaller droplets evaporate more

[DOI: 10.22068/ase.2024.694]

quickly, facilitating the molecular-level mixing of fuel and air.

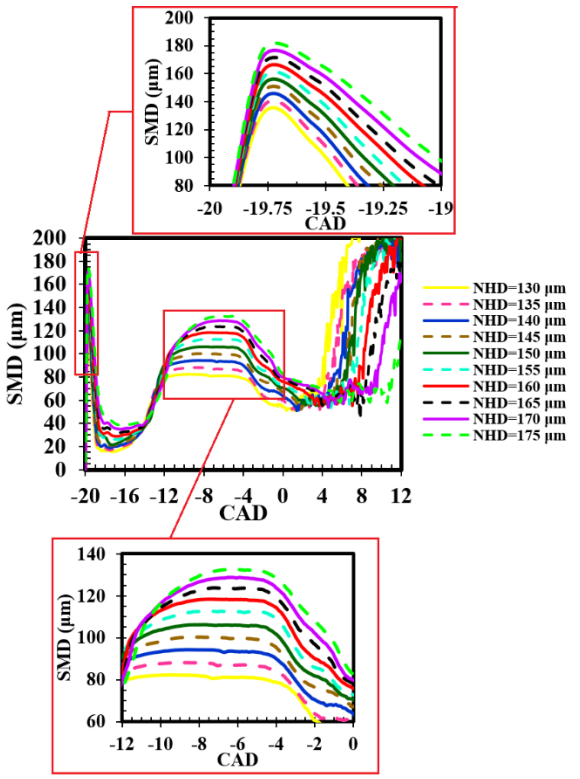

Figure 4: Effect of NHD on SMD

Reducing the SMD reduces the time and distance required for vaporization because smaller droplets convert to gas more quickly in a hot cylinder environment, resulting in more efficient combustion. With higher injection pressure and velocity, the shear forces on the fuel increase, breaking larger droplets into smaller droplets. Conversely, increasing the NHD increased the average droplet size because the shear forces were reduced in larger holes.

As previously discussed, reducing the NHD directly reduces the Sauter Mean Diameter (SMD) of the fuel droplets. This reduction results from the fuel breaking up into finer droplets, which significantly affects the number of droplets (NOD) produced and increases the droplet count. Figure 5 shows the effect of the NHD on the number of fuel droplets. The results show that smaller hole diameters result in a greater number of fuel droplets.

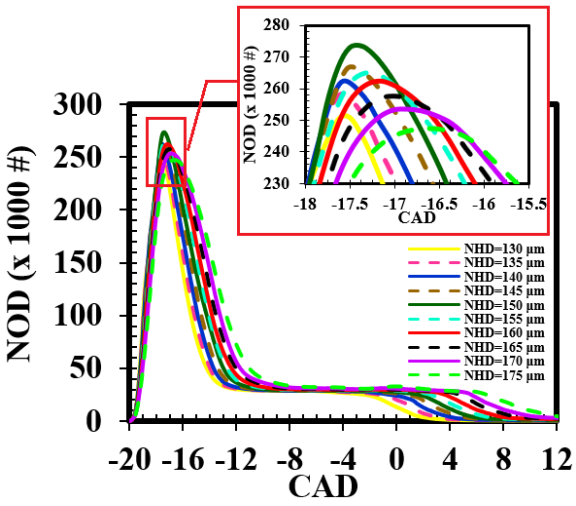

Figure 5: Effect of NHD on the NOD.

This increase in the NOD is accompanied by an increase in the total contact area between fuel and air, which plays a critical role in improving the mixing process and achieving a more uniform fuel distribution in the combustion chamber. These conditions allow for faster, more efficient, and more uniform combustion. From a physical and thermodynamic perspective, the increase in the NOD due to reduced SMD increases the droplet-to-volume ratio, which improves the evaporation rate of fuel. This improvement in evaporation reduces the time required to form a combustible mixture.

In contrast, increasing the hole diameter resulted in larger droplets and a reduced NOD, limiting the total contact area for mass and heat transfer. This situation increases the likelihood of fuel-rich regions and incomplete combustion, which directly leads to reduced combustion efficiency and higher emissions.

As previously discussed, the identification of minimum SMD points prior to the initial peak is critical for optimizing fuel evaporation and air-fuel mixing, which in turn enhances combustion efficiency and reduces emissions [46-48]. In these regions, fuel droplets are sufficiently small to evaporate rapidly and mix effectively with air, thereby promoting efficient combustion. As the injection process advances, the droplet size progressively decreases, further contributing to

[DOI: 10.22068/ase.2024.694]

the enhancement of combustion efficiency. The analysis of SMD values during the early stages of fuel injection offers crucial insights into the vaporization process, facilitating more precise control over air-fuel mixing. This methodology plays a pivotal role in improving combustion efficiency and mitigating greenhouse gas emissions, making it a key area of focus for researchers [49-52]. The Table 5 presents the results from Figures 4 and 5. It shows the maximum NOD, the CAD (Crank Angle Degree) at which the maximum NOD occurs, the maximum SMD, the CAD at which the maximum SMD is observed, the minimum SMD, and the CAD at which the minimum SMD occurs, for NHDs of 130 µm, 135, 150 µm, 160 µm, 165 µm, and 175 µm.

Table 5: Relationship between SMD, NOD, and CAD for NHDs of 130 µm, 135, 150 µm, 160 µm, 165 µm, and 175 µm.

NHD (µm)	Max NOD	Max NOD (deg) CAD	Max SMD (µm)	Max SMD (deg) CAD	Min SMD (µm)	Min SMD (deg) CAD
130	250913	-17.5	221.42	25.22	15.49	-17.34
135	258185	-17.56	230.86	18.32	16.92	-17.56
150	273498	-17.37	242.37	96.96	21.45	-17.37
160	262384	-17.18	255.03	102.45	28.7	-16.87
165	257634	-17.02	266.68	75.67	31.91	-16.53
175	247376	-16.55	273.12	73.33	38.24	-16.23

In the case of a nozzle diameter 150 µm (NHD 150), the number of fuel droplets reached 273498, indicating improved fuel dispersion within the combustion chamber. The maximum Sauter Mean Diameter (SMD) was observed to be 242.37 µm at a crank angle of 96.96°. Furthermore, the minimum SMD was found to be 21.45 µm at a crank angle of -17.37°, which occurs just before the initial peak of the SMD curve and is strategically chosen. This selection of the minimum SMD, especially during the early stages of injection, enhances fuel evaporation and fuel-air mixing, playing a crucial role in improving combustion efficiency.

In comparison to smaller nozzle diameters (130 and 135 µm), which produce fewer fuel droplets, nozzles with diameters of 150 and 160 µm provide significantly better dispersion, leading to more effective fuel-air mixing. This results in improved fuel evaporation and enhanced combustion efficiency. Additionally, when compared to larger nozzle diameters (165 and 175 µm), although the number of fuel droplets increases, the SMD values become notably larger, which may negatively impact the efficiency of fuel evaporation and fuel-air mixing.

In conclusion, nozzles with diameters of 150 and 160 µm optimally contribute to the fuel mixing and evaporation processes within the combustion chamber, yielding a significant improvement in combustion efficiency compared to both smaller and larger nozzles. These fuel droplets, particularly in the early stages of injection, effectively enhance the mixing process and can positively influence overall engine performance while reducing emissions.

As illustrated in Figure 6, the distribution and droplet size of fuel inside the combustion chamber depend on the diameter of the nozzle hole. The results for a range of angles show the effects of NHDs of 130 µm, 160 µm, and 175 µm.

The results demonstrate that the selection of the nozzle with a 130 µm hole diameter results in the observation of smaller droplets compared with the other nozzles, with a corresponding increase in the number of these droplets. This increase indicates pronounced spray break-up due to high shear force and injection pressure. This phenomenon increases the surface-to-volume ratio of the droplets, facilitating faster evaporation. Furthermore, the high fuel velocity exiting the nozzle generates additional shear force, which contributes to spray break-up and the formation of fine droplets. This resulted in a more uniform fuel distribution within the chamber. Furthermore, the fuel droplet

[DOI: 10.22068/ase.2024.694]

distribution was more uniform throughout all combustion stages, particularly in the vicinity of the TDC. At -15 aTDC, the fuel droplets are predominantly in the range of 10 µm to 30 µm, uniformly dispersed within the chamber. After these stages, at 1 aTDC and 15 aTDC, a decline in droplet size is observed, accompanied by an increase in the number of smaller droplets. This phenomenon indicates enhanced spray break-up and more effective air-fuel mixing.

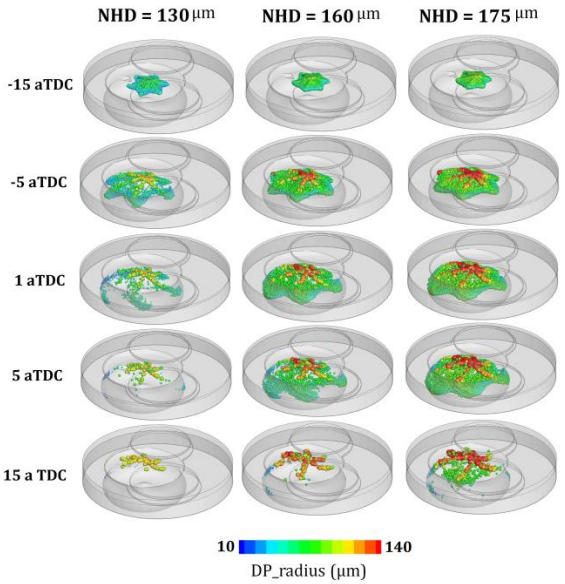

Figure 6: Droplet size distribution contours for different NHD 130 µm, 160 µm and 175 µm

However, as shown in this figure, the use of a 160 µm nozzle hole resulted in droplets with a mean diameter. This phenomenon can be attributed to the optimal equilibrium between the shear force, injection pressure, and spray break-up. The diameter of the fuel droplets is sufficient to facilitate their evaporation and effective mixing with air. Although injection velocity and pressure remain significant factors, they are not sufficiently high to produce excessively small droplets or cause an asymmetric distribution. The breakup of the spray was more controlled, achieving a balance between droplet count and size. Furthermore, the fuel distribution within the chamber demonstrates that the fuel is uniformly dispersed, contributing to the formation of a homogeneous mixture and reducing the probability of incomplete combustion. In this hole diameter, the fuel droplets exhibit a size ranging from 40 to 70 µm, suggesting larger sizes and reduced breakup. This could result in a longer NOD compared to the 130 µm NHD. In addition, the selection of a nozzle with a 175 µm hole diameter results in the production of larger droplets with fewer droplets. The reduced shear force and decreased injection pressure resulted in limited spray break-up, leading to the formation of larger droplets.

The spray dynamics have been changed in this NHD such that the injection velocity is reduced and the shear force is not sufficient to completely break the fuel droplets. The above conditions produce fuel-rich regions and diminished mixing. Furthermore, the distribution of droplets exhibits non-uniform, particularly in the vicinity of TDC, with a preponderance of larger droplets within the size range of 100 µm to 140 µm. This phenomenon can result in heightened HC and CO emissions, accompanied by a decrease in combustion efficiency.

As illustrated in Figure 7, the combustion temperature contours is presented for NHDs of 130 µm, 160 µm, and 175 µm at varying crank angles.

This figure analyzes the temperature distribution in the combustion chamber throughout the various combustion stages, with a particular focus on the impact of droplet size variations and the fuel-air mixing process at different crank angles. As demonstrated in the accompanying figure, the presence of a nozzle with a 130 µm hole diameter results in elevated temperatures and augmented hot regions within the combustion chamber, particularly in the vicinity of the TDC. This temperature increase was due to the faster evaporation of smaller droplets and more effective fuel-air mixing. Higher temperatures provide favorable conditions for the formation of NOx, which may increase these pollutants. In addition, combustion starts earlier than TDC in this case, resulting in a rise in the pressure and temperature before reaching the optimal value. This phenomenon can cause a decline in GIE efficiency and energy losses. Furthermore, the

[DOI: 10.22068/ase.2024.694]

analysis reveals that at crank angles of 5 aTDC and 15 aTDC, the temperature stabilizes within the higher range of 2500–2700 K, signifying complete combustion and effective energy release. At 15 aTDC, the temperature predominantly falls within the range 800–1200 K, signifying more complete combustion due to a more uniform fuel distribution.

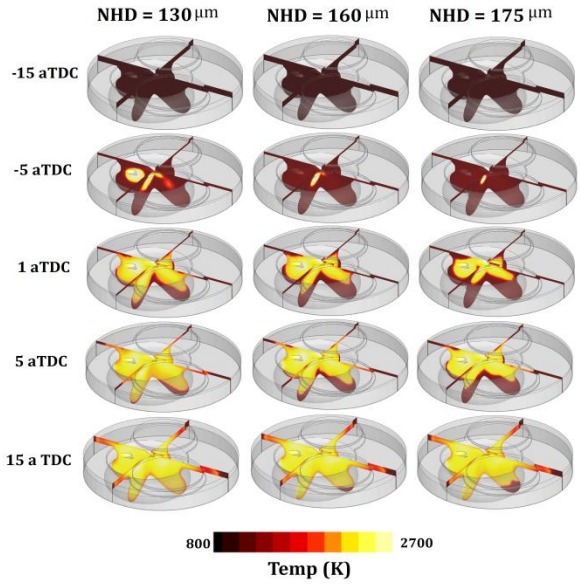

Figure 7: Combustion temperature contours for different NHD 130 µm, 160 µm and 175 µm

This figure demonstrates that the selection of holes with a diameter of 160 µm results in a more uniform temperature distribution and a reduced presence of hot and cold regions. The temperatures in proximity to TDC were found to be optimal, with the maximum temperature attained immediately after reaching the TDC. This optimal distribution reduces unnecessary heat transfer and enhances energy efficiency. Furthermore, it is evident that combustion starts at an appropriate time and is close to TDC. The peak pressure and temperature occur during the piston expansion stage, and they contribute to the high mechanical energy production.

Finally, the selection of a nozzle with a 175 µm hole diameter resulted in the observation of colder regions in the combustion chamber, indicating slower evaporation and insufficient mixing. Lower temperatures increase the likelihood of incomplete combustion, leading to higher HC and CO emissions. Furthermore, the combustion process was delayed, with a substantial portion of the combustion occurring during the piston expansion stroke. This delay in combustion reduces efficiency and a reduction in the pressure and temperature of the chamber. At 15 aTDC, the temperature has not yet reached a peak, indicating reduced combustion efficiency.

Figure 8 illustrates the variations in NOD, start of combustion (SOC), and combustion duration for different NHD. The results indicate that reducing the NHD significantly affects the combustion process. Smaller nozzle diameters result in shorter NODs because of the production of smaller fuel droplets and improved fuel-air mixing. Smaller droplets with greater surface area evaporate faster and form a combustible mixture in a shorter time. This reduction in the evaporation and mixture formation times reduces the NOD and optimizes the combustion timing.

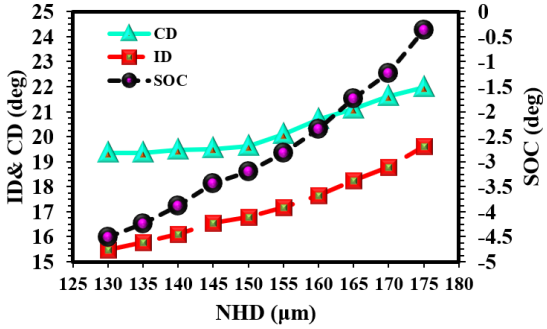

Figure 8: NOD, combustion duration, and NOD for various NHD

Moreover, the improved atomization and reduction in the Sauter Mean Diameter (SMD) of fuel droplets resulted in a shorter pre-mixed combustion phase. These changes lead to a faster start of combustion and shorter overall combustion duration. The combustion start is a critical factor in determining the performance of internal combustion engines and significantly affects efficiency and energy production. If the NOD occurs before the piston reaches the top

[DOI: 10.22068/ase.2024.694]

dead center (TDC), it can lead to increased cylinder pressure and temperature before TDC, resulting in incomplete combustion and lower energy output. This phenomenon causes energy losses and reduces engine efficiency.

To achieve optimal engine performance, it is essential to synchronize the NOD with the piston's approach to the top dead center (TDC). This ensures that the peak pressure and temperature occur during the piston's downward motion, thereby maximizing the energy generation and mechanical efficiency. Consequently, precise control of combustion timing is imperative for enhancing engine efficiency and improving overall performance [53, 54].

On the other hand, increasing the diameter of the nozzle hole has opposite effects. Larger droplets require more time for evaporation and fuel-air mixing, leading to an increase in NOD. Furthermore, an increase in the NHD decreases the combustion speed and an increase in the combustion uniformity, thereby extending the combustion duration. This prolonged duration can reduce combustion efficiency and increase pollutant emissions, as there is reduced opportunity for complete combustion under optimal conditions.

The variation in the injector NHD plays a crucial role in influencing the key combustion parameters, including the cylinder pressure, temperature, heat release rate (HRR), and cumulative heat release (CHR), as depicted in Figure 9. The results indicate that decreasing the NHD results in enhanced fuel atomization and improved fuel-air mixing, leading to accelerated and more complete combustion. Consequently, the peak pressure and temperature within the cylinder increase, and chemical reactions occur more efficiently. For smaller nozzle diameters, the onset and peak of pressure and temperature occur earlier due to the accelerated evaporation of smaller fuel droplets and the expedited ignition process.

Despite these advantages, the early occurrence of peak pressure and temperature has potential drawbacks. Combustion before the top dead center (TDC) generates part of the released energy to overcome the opposing piston pressure rather than producing useful work. This mechanical loss can reduce thermal efficiency. Therefore, improper combustion timing with reduced NHD may adversely affect the overall engine performance.

In contrast, increasing the NHD reduced the intensity of fuel atomization and resulted in less uniform fuel-air mixing. This change reduces the local fuel-air density and consequently the peak cylinder pressure and temperature. Combustion under these conditions was more uniform, with fewer hotspots observed. Additionally, larger nozzle diameters lead to a lower peak HRR and a delayed occurrence of this peak, which can be attributed to the extended fuel-air mixing time.

The variation in the NHD significantly affects the fuel flow characteristics and the combustion process. A higher fuel flow velocity through nozzles with smaller hole diameters results in greater turbulence in the combustion chamber. Smaller fuel droplets due to higher injection velocity generate more turbulence in the flow field, and turbulent flows effectively enhance fuel-air mixing. Although this initially improves the combustion process, at very high values, it may lead to combustion instability and increased heat transfer [55-57].

As illustrated in Figure 10, the variation in the NHD exerts an influence on TKE (turbulent kinetic energy). The results indicate that reducing the NHD increases the TKE because the fuel spray generates more turbulence in the flow. This phenomenon is attributed to the higher fuel flow velocity, as demonstrated in the "flow velocity" diagram. This increase in turbulent energy, in turn, promotes better fuel-air mixing and enhances combustion. Conversely, an increase in the NHD decreases the fuel exit velocity from the nozzle, reducing the TKE. This reduction can be attributed to the diminished fuel flow velocity in the larger nozzles, which, in turn, reduces the flow turbulence.

[DOI: 10.22068/ase.2024.694]

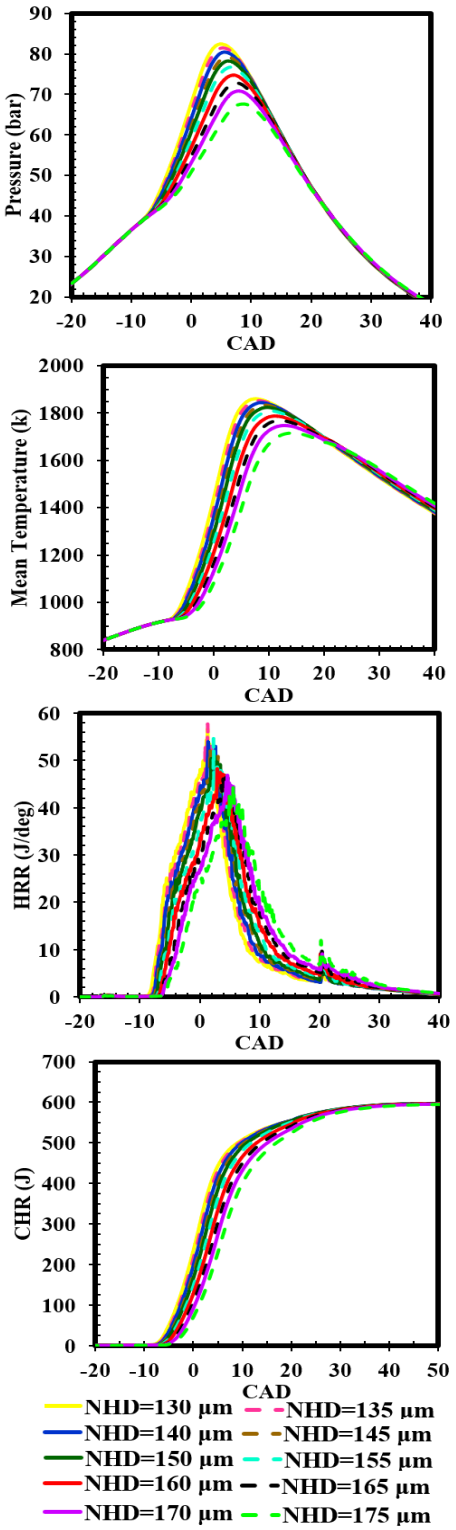

Figure 9: Effects of different NHD on in-cylinder Pressure, temperature, HRR, and CHR

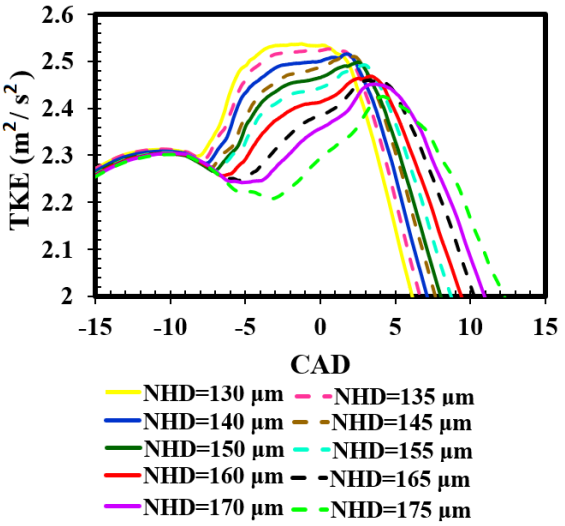

Figure 10: Effect of NHD on TKE.

In smaller nozzles, the higher flow velocity and greater shear force produce higher turbulent energy, resulting in better fuel-air mixing and, consequently, faster and more uniform combustion. In contrast, in larger nozzles, due to the reduced fuel velocity, mixing may be incomplete, and fuel may disperse and evaporate inefficiently. Moreover, the reduction in turbulent energy could negatively affect fuel-air mixing, leading to a decline in combustion quality. Additionally, the decrease in TKE can reduce the opportunities for mass and energy transfer between the fuel flow and the surrounding air, ultimately resulting in decreased combustion process efficiency.

The variation in the NHD significantly affects the fuel-air mixing process. Studies have shown that mixing time is dependent on SMD (Sauter Mean Diameter) and injection conditions [58, 59]. Figure 11 illustrates the mixing time as a function of the nozzle-hole diameter. The results show that decreasing the NHD reduces the mixing time. This is due to the faster evaporation of smaller fuel droplets, which have a larger surface area in contact with air, allowing for quick mixing. As a result, the mixing process is facilitated, thereby reducing the mixing time. In contrast, larger NHDs produce larger droplets, which require more time for the droplets to evaporate. This increases fuel-air mixing time.

[DOI: 10.22068/ase.2024.694]

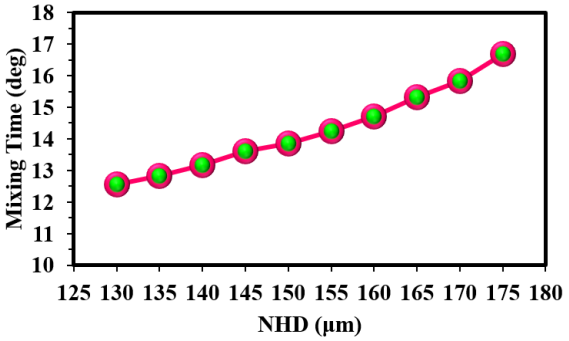

Figure 11: Mixing time under various NHD

As shown in Figure 12, the variation in the NHD exerts a substantial influence on the process of heat transfer. The results indicate that decreasing the diameter of the nozzle holes enhances the heat transfer rate. This phenomenon is attributed to the production of smaller fuel droplets, which results in an increased surface area in contact with the hot gases in the combustion chamber. The increased surface contact enhances the heat transfer, thereby improving the energy efficiency. Additionally, higher pressure and temperature during the combustion process also contribute to improved heat transfer rates, as the hotter gases in the combustion chamber have a greater capacity to transfer energy to fuel droplets. However, excessive heat transfer can lower the chamber temperature and create cold regions within the combustion chamber, ultimately reducing the efficiency. This phenomenon may negatively affect engine performance, particularly the combustion process [60-63].

In contrast, increasing the NHD generally reduces the heat transfer rate. This reduction is due to the decrease in the turbulent kinetic energy (TKE) and the reduced contact area between the fuel and the hot air inside the cylinder. In smaller nozzles hole, the higher turbulence and better fuel-air mixing result in more effective heat transfer. Conversely, in larger nozzles, larger fuel droplets evaporate more slowly, reducing their ability to transfer heat to hot gases. This heat transfer reduction can lead to decreased temperature uniformity within the combustion chamber, resulting in lower engine efficiency.

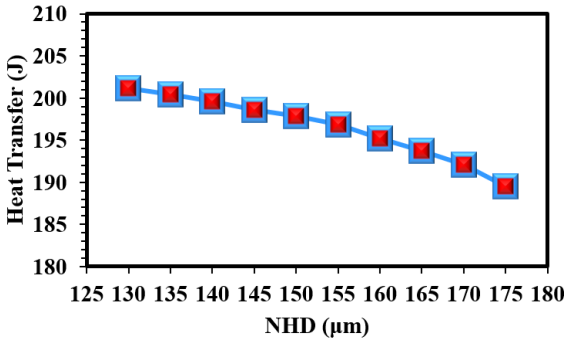

Figure 12: Heat transfer under different NHD

Figure 13 presents the variation in combustion efficiency and gross indicated efficiency (GIE) as a function of NHD in an RCCI engine. At the baseline NHD of 165 µm, combustion efficiency and GIE were 91.92% and 38.57%, respectively. This baseline serves as a reference point for evaluating the impact of increasing and decreasing the NHD.

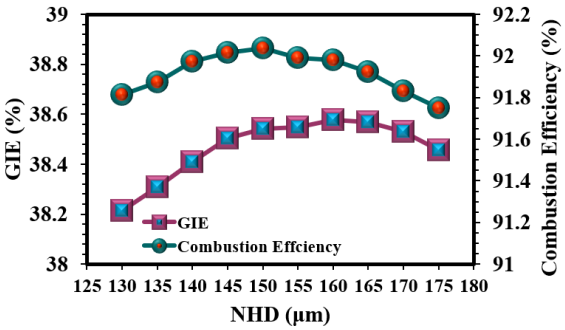

Figure 13: GIE and combustion efficiency at various NHD

At The results reveal that the maximum combustion efficiency of 92.04% occurs at a NHD of 150 µm, representing an increase of 0.12% compared to the baseline. This improvement is attributed to the optimization of fuel spray dynamics, where the droplet size and distribution enhance evaporation and fuel-air mixing, leading to more complete combustion. Similarly, the highest GIE of 38.58% is achieved

[DOI: 10.22068/ase.2024.694]

at a NHD of 160 μm, a 0.01% increase compared to the baseline. This minor improvement highlights the sensitivity of GIE to small variations in nozzle diameter, which optimize the timing of energy release and reduce energy losses.

A reduction in the NHD to 130 μm results in combustion efficiency and GIE values of 91.81% and 38.21%, respectively. This decline indicates suboptimal spray dynamics characterized by smaller droplet sizes and higher injection velocity, which can lead to premature ignition. Premature ignition reduces the effective combustion duration, resulting in incomplete energy utilization and lower efficiencies.

Conversely, increasing the NHD to 175 μm leads to a combustion efficiency of 91.75% and a GIE of 38.46%. These reductions are primarily due to the formation of larger fuel droplets, which prolong evaporation time and hinder effective fuel-air mixing. The delayed evaporation also causes combustion to occur later in the expansion stroke, increasing heat losses and decreasing efficiency.

The analysis underscores the critical role of nozzle design in determining spray dynamics, evaporation behavior, and combustion performance. Optimal nozzle diameters (150–160 μm) balance key processes such as droplet breakup, evaporation timing, and mixing efficiency, thereby maximizing combustion and energy utilization. Deviations from these optimal diameters disrupt this balance, leading to either incomplete combustion in larger nozzles or premature ignition in smaller nozzles, both of which negatively impact efficiency.

These findings demonstrate that NHD is a pivotal parameter in enhancing engine performance and minimizing energy losses, emphasizing its importance in the design and optimization of RCCI engines.

Overall, the findings indicate that deviations from the optimal NHD disrupt the balance of key processes such as droplet size distribution, evaporation timing, and fuel-air mixing. These imbalances either lead to premature ignition in smaller nozzles or incomplete combustion in larger nozzles, both of which negatively impact efficiency and emissions performance [64, 65].

The impact of the NHD on the HC, CO, and NOx emissions is illustrated in Figure 14. The results demonstrate that variations in NHD significantly influence pollutant emissions. Specifically, at the baseline NHD of 165 μm, NOx emissions were recorded at 4.33 gr/kw.h. When the nozzle diameter was reduced to 130 μm (the smallest diameter) and increased to 175 μm (the largest diameter), NOx emissions increased to 10.08 gr/kw.h and decreased to 2.66 gr/kw.h, respectively. These findings indicate that the minimum NOx emissions occurred with the 175 μm diameter, yielding 2.66 gr/kw.h. Furthermore, reducing the nozzle diameter from 165 μm to 130 μm resulted in a 5.76 gr/kw.h increase in NOx emissions, while increasing the diameter to 175 μm led to a decrease of 1.67 gr/kw.h in NOx emissions.

In terms of HC emissions, at the baseline diameter of 165 μm, the HC emissions were 14.85 gr/kw.h. With a reduction in nozzle diameter to 130 μm, HC emissions increased slightly to 14.99 gr/kw.h, and with an increase to 175 μm, HC emissions rose further to 15.27 gr/kw.h. The lowest HC emissions were observed at a nozzle diameter of 150 μm, where emissions were 14.55 gr/kw.h. The reduction in nozzle diameter from 165 μm to 130 μm resulted in a 0.14 gr/kw.h increase in HC emissions, while increasing the diameter to 175 μm led to a 0.43 gr/kw.h rise in HC emissions.

For CO emissions, at the baseline diameter of 165 μm, CO emissions were 3.93 gr/kw.h. With a reduction to 130 μm, CO emissions decreased to 3.65 gr/kw.h, whereas with an increase to 175 μm, CO emissions increased to 4.22 gr/kw.h. The minimum CO emissions were recorded at a nozzle diameter of 135 μm, where emissions were 3.62 gr/kw.h. Reducing the nozzle diameter from 165 μm to 130 μm led to a 0.28 gr/kw.h reduction in CO emissions, while increasing the diameter to 175 μm resulted in a 0.29 gr/kw.h increase in CO emissions.

[DOI: 10.22068/ase.2024.694]

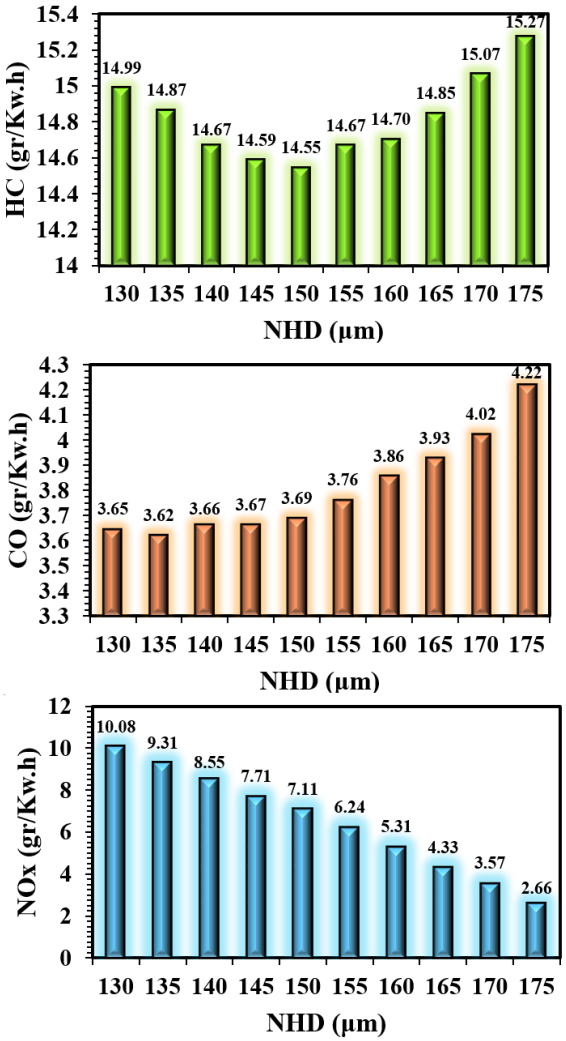

Figure 14: Comparison of HC, CO, and NOx emissions for different NHD

These findings shows that a smaller nozzle diameter tends to elevate combustion temperatures, improving combustion efficiency and thereby reducing HC and CO emissions. However, this approach also leads to an increase in NOx emissions due to the higher temperatures favoring NOx formation. Conversely, a larger nozzle diameter reduces combustion temperature, which results in lower NOx emissions but increases HC and CO emissions due to incomplete combustion. This analysis highlights the importance of selecting an optimal NHD, as it involves a delicate balance between fuel-air mixing quality, combustion temperature, and pollutant emissions.

5. Conclusion

This study comprehensively examined the effect of nozzle hole diameter (NHD) on spray dynamics, combustion performance, and emission characteristics in a 1.9-liter RCCI engine. Through CFD simulations, the impact of varying NHDs (130–175 µm) was analyzed on critical parameters such as droplet size, evaporation rate, turbulent kinetic energy (TKE), combustion efficiency, and pollutant emissions. The results highlight the significance of optimizing NHD to achieve a balance between engine performance and environmental objectives.

1. Spray Dynamics and Atomization

Smaller NHDs (e.g., 130 µm) significantly improved atomization, reducing the Sauter Mean Diameter (SMD) to 15.49 µm and increasing the droplet count by 24%. These changes enhanced evaporation and mixing, leading to faster combustion and more uniform fuel-air distribution.

Larger NHDs (e.g., 175 µm), however, resulted in larger droplets, slower evaporation rates, and non-uniform mixing, which negatively impacted combustion quality and emission levels.

2. Combustion Performance

Optimal NHDs (150–160 µm) achieved the highest combustion efficiency (92.04%) and gross indicated efficiency (38.58%) by balancing spray breakup, droplet size, evaporation timing, and mixing uniformity.

Smaller NHDs caused premature ignition and higher energy losses, while larger NHDs delayed combustion, lowering peak cylinder pressure and temperature and reducing efficiency.

3. Emission Trade-offs

Smaller NHDs increased NOx emissions to 10.08 g/kWh due to elevated in-cylinder temperatures, despite improving combustion efficiency.

[DOI: 10.22068/ase.2024.694]

Larger NHDs reduced NOx emissions to 2.66 g/kWh but led to higher HC (15.27 g/kWh) and CO (4.22 g/kWh) emissions, primarily due to incomplete combustion caused by insufficient mixing.

4. Key Relationships and Dynamics

Optimal mixing and evaporation were observed when SMD values were minimized in the early stages of fuel injection. This emphasizes the importance of analyzing SMD behavior and droplet distribution contours to optimize combustion processes and reduce emissions.

Turbulent kinetic energy (TKE) played a pivotal role in enhancing uniform mixing; however, excessive TKE in smaller NHDs caused combustion instability, while larger NHDs lacked adequate turbulence for effective mixing and evaporation.

Final Insights

The findings identify an optimal NHD range of 150–160 μm, which effectively balances spray dynamics, combustion efficiency, and emission characteristics. Smaller diameters offer enhanced atomization and mixing but present challenges with premature ignition and elevated NOx emissions. Conversely, larger diameters mitigate NOx emissions but compromise combustion efficiency due to delayed evaporation and incomplete combustion.

These results underscore the critical role of nozzle geometry in RCCI engine optimization. Future research should focus on advanced injector technologies, adaptive nozzle designs, and alternative fuel integration to enhance adaptability and efficiency across a broader range of operating conditions. By addressing these aspects, the potential for further reducing emissions and improving engine performance can be fully realized.

List of symbols

Nomenclature

t	Time (s)
u	Velocity (m/s)
S	Thermal energy source (W/Kg)
Y	Mass fraction
D	Diffusivity coefficient
e	Specific internal energy (J/Kg)
K	Thermal conductivity (W/m. K)
h	Specific enthalpy (J/Kg)
P	Pressure (Pa)
V	Volume (m^3)
T	Temperature (K)
Q	Heat (J)
m	Mass (Kg)
U	Internal energy (J)
s	Entropy (J/K)
h	Enthalpy (J/Kg)
G	Gibbs energy (J/Kg)
R	Ideal gas constant (J/mol K)
W	Work (J)

Abbreviations

GIE	Gross Indicated Efficiency (%)
HRR	Heat Release Rate (J/deg)
CHR	Cumulative Heat Release (J)
CA	Crank Angle
CAD	Crank Angle Degree
CA10	Crank angle of 10% heat released
CA50	Crank angle of 50% heat released
CA90	Crank angle of 90% heat released
LTC	Low-temperature combustion
SI	Spark Ignition
CI	Compression Ignition
HCCI	Homogeneous Charge-Compression Ignition
RCCI	Reactivity-Controlled Compression

[DOI: 10.22068/ase.2024.694]

	Ignition
CO	Carbon monoxide
CO_2	Carbon dioxide
NOx	Nitrogen oxide
HC	Hydrocarbons
EGR	Exhaust Gas Recirculation
PM	Particulate matter
IMEP	Indicated Mean Effective Pressure
BMEP	Brake Mean Effective Pressure
SOI	Start Of Injection
SOC	Start of combustion
ICE	Internal combustion engine
IVC	Inlet valve closing
EVO	Exhaust valve opening
BDC	Bottom dead center
aTDC	After the top dead center
bTDC	Before the top dead center
CFD	Computational Fluid Dynamics
DDM	Droplet distinct Model
KH-RT	Kelvin-Helmholtz-Rayleigh-Taylor
RNG	Re-Normalization Group
NTC	Nutation Time Constant
AMR	Adaptive Mesh Refinement
SMD	Sauter Mean Diameter
TKE	Turbulence kinetic energy
LHV	Lower heating value (MJ/kg)
RPM	Revolutions per minute
NG	Natural gas
BR	Brake Thermal Efficiency (%)
NHD	Nozzle Hole Diameter (μm)
NOD	Number Of Droplets
ID	Ignition Delay (deg)
CD	Combustion Duration (deg)
ID	Ignition Delay (deg)

References

[1] M.J. Noroozi, M. Seddiq, H. Habibi, Investigation of the Effects of Diesel Injection Strategies in a Reactivity Controlled Dieseliso-Butanol Compression Ignition Engine, Automotive Science and Engineering, 10 (2020) 3470-3394.

[2] B. Borjian Fard, A. Gharehghani, B. Bahri, Modeling and optimization of diesel-natural gas RCCI engine performance, combustion noise and emissions using response surface method, Automotive Science and Engineering, 11 (2021) 3547-3559.

[3] A. Kakaee, P. Rahnama, A. Paykani, Numerical study of reactivity controlled compression ignition (RCCI) combustion in a heavy-duty diesel engine using 3D-CFD coupled with chemical kinetics, International Journal of Automotive Engineering, 4 (2014) 792-804.

[4] A. Paykani, H. Chehrmonavari, A. Tsolakis, T. Alger, W.F. Northrop, R.D. Reitz, Synthesis gas as a fuel for internal combustion engines in transportation, Progress in Energy and Combustion Science, 90 (2022) 100995.

[5] Y. Tang, D. Lou, C. Wang, P.-q. Tan, Z. Hu, Y. Zhang, L. Fang, Study of visualization experiment on the influence of injector nozzle diameter on diesel engine spray ignition and combustion characteristics, Energies, 13 (2020) 5337.

[6] A.R. Andsaler, A. Khalid, N.S.A. Abdullah, A. Sapit, N. Jaat, The effect of nozzle diameter, injection pressure and ambient temperature on spray characteristics in diesel engine, in: Journal of Physics: Conference Series, Vol. 822, IOP Publishing, 2017, pp. 012039.

[7] S. Som, A.I. Ramirez, D.E. Longman, S.K. Aggarwal, Effect of nozzle orifice geometry on spray, combustion, and emission characteristics under diesel engine conditions, Fuel, 90 (2011) 1267-1276.

[DOI: 10.22068/ase.2024.694]

[8] O. Klyus, M. Szczepanek, G. Kidacki, P. Krause, S. Olszowski, L. Chybowski, The Effect of Internal Combustion Engine Nozzle Needle Profile on Fuel Atomization Quality, Energies, 17 (2024) 266.

[9] Y. Liu, W. Su, The Influence of Injector Nozzle Diameter on High-Density and Lean Mixture Combustion in Heavy-Duty Diesel Engines, Energies, 17 (2024) 2549.

[10] H. Dave, B. Sutaria, B. Patel, Influence of nozzle hole diameter on combustion and emission characteristics of diesel engine under pilot injection mode, in: IOP Conference Series: Materials Science and Engineering, Vol. 810, IOP Publishing, 2020, pp. 012041.

[11] J. Zheng, J. Wang, Z. Zhao, D. Wang, Z. Huang, Effect of equivalence ratio on combustion and emissions of a dual-fuel natural gas engine ignited with diesel, Applied Thermal Engineering, 146 (2019) 738-751.

[12] V. Singh, N. Kumar, Numerical investigation of the effect of nozzle hole diameter on the combustion, emission, and spray characteristics in a diesel engine, Energy Sources, Part A: Recovery, Utilization, and Environmental Effects, (2021) 1-18.

[13] M. Zubel, B. Lehrheuer, S. Pischinger, Impact of increased injector nozzle hole diameters on engine performance, exhaust particle distribution and methane and formaldehyde emissions during dimethyl ether operation, International Journal of Engine Research, 22 (2021) 503-515.

[14] X. Wang, Z. Huang, W. Zhang, O.A. Kuti, K. Nishida, Effects of ultra-high injection pressure and micro-hole nozzle on flame structure and soot formation of impinging diesel spray, Applied Energy, 88 (2011) 1620-1628.

[15] C. Yao, P. Geng, Z. Yin, J. Hu, D. Chen, Y. Ju, Impacts of nozzle geometry on spray combustion of high pressure common rail injectors in a constant volume combustion chamber, Fuel, 179 (2016) 235-245.

[16] W. Zhao, J. Pan, H. Wei, L. Chen, Synergy effect of nozzle structure and pre-chamber reactivity on the combustion characteristics of ammonia engines, Fuel, 381 (2025) 133360.

[17] R. Payri, F.J. Salvador, J. Gimeno, J. De la Morena, Effects of nozzle geometry on direct injection diesel engine combustion process, Applied Thermal Engineering, 29 (2009) 2051-2060.

[18] L. Fu, J. Zhu, Z. Liu, X. Liu, J. Chen, L. Guo, Z. Li, Z. Wang, Study on the effects of hydrogen nozzle diameter on the combustion and emission characteristics of hydrogen-blended methanol engines, International Journal of Hydrogen Energy, 69 (2024) 39-50.

[19] Z. Zhang, C. Zhao, Z. Xie, F. Zhang, Z. Zhao, Study on the effect of the nozzle diameter and swirl ratio on the combustion process for an opposed-piston two-stroke diesel engine, Energy Procedia, 61 (2014) 542-546.

[20] E.V. Rojas-Reinoso, K. Morales-Chauca, J. Lara-Lara, J.A. Soriano, R. García-Contreras, Adaptation and Validation of Injection Rate Predictive Model for Solenoid Type Injectors with Different Nozzle Geometry, Applied Sciences, 14 (2024) 3394.

[21] S. Lahane, K. Subramanian, Impact of nozzle holes configuration on fuel spray, wall impingement and NOx emission of a diesel engine for biodiesel–diesel blend (B20), Applied Thermal Engineering, 64 (2014) 307-314.

[22] I. Naruemon, L. Liu, Q. Mei, Y. Wu, X. Ma, K. Nishida, Investigating the effects of split injection with different injection patterns on diesel spray mixing, Frontiers in Energy Research, 10 (2023) 933591.

[23] S.K. Amedorme, J. Apodi, A Computational Fluid Dynamics-based Correlation to Predict Droplet Sauter Mean Diameter for?? Yliq Atomization Model in Pressure Swirl Atomizer, European Journal of Engineering and Technology Research, 6 (2021) 69-76.

[DOI: 10.22068/ase.2024.694]

[24] Y. Kim, K. Kim, K. Lee, Effect of a 2-stage injection strategy on the combustion and flame characteristics in a PCCI engine, International Journal of Automotive Technology, 12 (2011) 639-644.

[25] Z. Yue, R.D. Reitz, An equilibrium phase spray model for high-pressure fuel injection and engine combustion simulations, International Journal of Engine Research, 20 (2019) 203-215.

[26] S. Yokoi, S. Sugawara, R. Sagawa, Y. Saito, Y. Matsushita, H. Aoki, Experimental investigation of atomization and combustion characteristics of high-pressure pulse sprays, Fuel Processing Technology, 148 (2016) 269-275.

[27] S.H. Park, J. Cha, C.S. Lee, Reduction of the pollutant emissions from a diesel engine by the application of dimethyl ether (DME) and the control of the intake oxygen flow rate, Energy & fuels, 26 (2012) 3024-3033.

[28] A. Rahimi, E. Fatehifar, R.K. Saray, Development of an optimized chemical kinetic mechanism for homogeneous charge compression ignition combustion of a fuel blend of n-heptane and natural gas using a genetic algorithm, Proceedings of the institution of mechanical engineers, Part D: Journal of Automobile Engineering, 224 (2010) 1141-1159.

[29] J.K. Dukowicz, A particle-fluid numerical model for liquid sprays, Journal of computational Physics, 35 (1980) 229-253.

[30] D.P. Schmidt, C.J. Rutland, A new droplet collision algorithm, Journal of computational Physics, 164 (2000) 62-80.

[31] J.C. Beale, R.D. Reitz, Modeling spray atomization with the Kelvin-Helmholtz/Rayleigh-Taylor hybrid model, Atomization and sprays, 9 (1999).

[32] Z. Han, R.D. Reitz, Turbulence modeling of internal combustion engines using RNG κ-ε models, Combustion science and technology, 106 (1995) 267-295.

[33] S.L. Post, J. Abraham, Modeling the outcome of drop–drop collisions in Diesel sprays, International Journal of Multiphase Flow, 28 (2002) 997-1019.

[34] P.J. O'Rourke, A. Amsden, A spray/wall interaction submodel for the KIVA-3 wall film model, SAE transactions, (2000) 281-298.

[35] M. Raju, M. Wang, M. Dai, W. Piggott, D. Flowers, Acceleration of detailed chemical kinetics using multi-zone modeling for CFD in internal combustion engine simulations, in, SAE Technical Paper, 2012.

[36] M. Nazemi, Modeling and analysis of reactivity controlled compression ignition (RCCI) combustion, in, Michigan Technological University, 2015.

[37] M. Nazemian, E. Neshat, R.K. Saray, Effects of piston geometry and injection strategy on the capacity improvement of waste heat recovery from RCCI engines utilizing DOE method, Applied Thermal Engineering, 152 (2019) 52-66.

[38] K. Poorghasemi, R. Khoshbakhti Saray, E. Ansari, S.M. Mousavi, A. Zehni, Statistical analysis on the effect of premixed ratio, EGR, and diesel fuel injection parameters on the performance and emissions of a NG/Diesel RCCI engine using a DOE method, Proceedings of the institution of mechanical engineers, Part D: Journal of Automobile Engineering, 236 (2022) 460-473.

[39] P. Rahnama, A. Paykani, V. Bordbar, R.D. Reitz, A numerical study of the effects of reformer gas composition on the combustion and emission characteristics of a natural gas/diesel RCCI engine enriched with reformer gas, Fuel, 209 (2017) 742-753.

[40] P. Rahnama, A. Paykani, R.D. Reitz, A numerical study of the effects of using hydrogen, reformer gas and nitrogen on

[DOI: 10.22068/ase.2024.694]

combustion, emissions and load limits of a heavy duty natural gas/diesel RCCI engine, Applied Energy, 193 (2017) 182-198.

[41] K. Poorghasemi, R.K. Saray, E. Ansari, B.K. Irdmousa, M. Shahbakhti, J.D. Naber, Effect of diesel injection strategies on natural gas/diesel RCCI combustion characteristics in a light duty diesel engine, Applied Energy, 199 (2017) 430-446.

[42] A.-H. Kakaee, A. Nasiri-Toosi, B. Partovi, A. Paykani, Effects of piston bowl geometry on combustion and emissions characteristics of a natural gas/diesel RCCI engine, Applied Thermal Engineering, 102 (2016) 1462-1472.

[43] S.S. Kumaran, P. Raghu, Effect of Nozzle Hole Number on Diesel Engine Using Diesel and Biodiesel Blends, in: IOP Conference Series: Materials Science and Engineering, Vol. 912, IOP Publishing, 2020, pp. 042007.

[44] Y. Nakahama, K. Takahashi, Effect of gas injection pattern on magnetically expanding rf plasma source, Japanese Journal of Applied Physics, 63 (2024) 09SP01.

[45] F.J. Martos, J.A. Soriano, C. Mata, O. Armas, F. Soto, Impact of alternative and fossil diesel fuels on internal flow of injection nozzle, International Journal of Engine Research, 23 (2022) 940-957.

[46] J.-Y. Koo, J.K. Martin, Droplet sizes and velocities in a transient diesel fuel spray, SAE transactions, (1990) 929-947.

[47] N. Fdida, J.-B. Blaisot, A. Floch, D. Dechaume, Drop-size measurement techniques applied to gasoline sprays, Atomization and sprays, 20 (2010).

[48] P. Stężycki, M. Kowalski, A. Jankowski, Z. Sławinski, Laser research of the fuel atomization process of internal combustion engines, Наука и техника, (2020) 34-42.

[49] N. Chideme, P. De Vaal, Effect of Liquid Viscosity and Surface Tension on the Spray Droplet Size and the Measurement Thereof, Journal of Applied Fluid Mechanics, 17 (2024) 2652-2672.

[50] N. Sharma, W.D. Bachalo, A.K. Agarwal, Spray droplet size distribution and droplet velocity measurements in a firing optical engine, Physics of Fluids, 32 (2020).

[51] T. Yamashita, D. Matsuda, I. Kimura, K. Nishimura, E. Matsumura, J. Senda, Droplet Breakup Model in Spray Combustion SimulationBased on Measurements of Droplet Disintegration Mechanisms, International Journal of Automotive Engineering, 13 (2022) 155-162.

[52] B.P. Sangeorzan, O.A. Uyehara, P.S. Myers, Time-resolved drop size measurements in an intermittent high-pressure fuel spray, SAE transactions, (1984) 988-1006.

[53] S. Lee, G. Kim, C. Bae, Effect of injection and ignition timing on a hydrogen-lean stratified charge combustion engine, International Journal of Engine Research, 23 (2022) 816-829.

[54] X. Huin, M. Di Loreto, E. Bideaux, H. Benzaoui, Improving performance specifications of internal combustion engine dedicated to plug-in hybrid electric vehicles based on coupled optimization methodology, Transactions of the Institute of Measurement and Control, (2021) 01423312211029692.

[55] S. Hisham Amirnordin, S. Ismail, R. Yii Shi Chin, N. Mansor, M. Fawzi, A. Khalid, Effects of Nozzle Diameter on the Spray Characteristics of Premix Injector in Burner System, Applied Mechanics and Materials, 773 (2015) 570-574.

[56] M.B. Ahmed, M.W. Mekonen, Effects of injector nozzle number of holes and fuel injection pressures on the diesel engine characteristics operated with waste cooking oil biodiesel blends, Fuels, 3 (2022) 275-294.

[57] X. Li, Y. Cheng, S. Ji, X. Yang, L. Wang, Sensitivity analysis of fuel injection

[DOI: 10.22068/ase.2024.694]

characteristics of GDI injector to injector nozzle diameter, Energies, 12 (2019) 434.

[58] Y. Feng, H. Wang, R. Gao, Y. Zhu, A zero-dimensional mixing controlled combustion model for real time performance simulation of marine two-stroke diesel engines, Energies, 12 (2019) 2000.

[59] F. Maroteaux, E. Mancaruso, B.M. Vaglieco, A Mixing Timescale Model for PDF Simulations of LTC Combustion Process in Internal Combustion Engines, in, SAE Technical Paper, 2019.

[60] S. Moser, K.D. Edwards, T. Schoeffler, Z. Filipi, CFD/FEA Co-simulation framework for analysis of the thermal barrier coating design and its impact on the HD diesel engine performance, Energies, 14 (2021) 2044.

[61] P. Andruskiewicz, P. Najt, R. Durrett, S. Biesboer, T. Schaedler, R. Payri, Analysis of the effects of wall temperature swing on reciprocating internal combustion engine processes, International Journal of Engine Research, 19 (2018) 461-473.

[62] V. Manente, P. Tunestål, B. Johansson, Influence of the wall temperature and combustion chamber geometry on the performance and emissions of a mini HCCI engine fueled with diethyl ether, in, SAE Technical Paper, 2008.

[63] M. Pucilowski, M. Jangi, S. Shamun, M. Tuner, X.-S. Bai, Heat Loss Analysis for Various Piston Geometries in a Heavy-Duty Methanol PPC Engine, in, SAE Technical Paper, 2018.

[64] M. Walle Mekonen, N. Sahoo, Combined effects of fuel injection pressure and injector nozzle holes on the performance of preheated palm oil methyl ester used in a diesel engine, Biofuels, 11 (2020) 19-35.

[65] S. Kang, S. Lee, D. Hong, C. Bae, Effects of nozzle orifice diameter and hole number on diesel combustion and engine performance, International Journal of Automotive Technology, 23 (2022) 481-494.

[DOI: 10.22068/ase.2024.694]